UNIVERSITY OF CRETE

GRADUATE PROGRAM IN NEUROSCIENCES

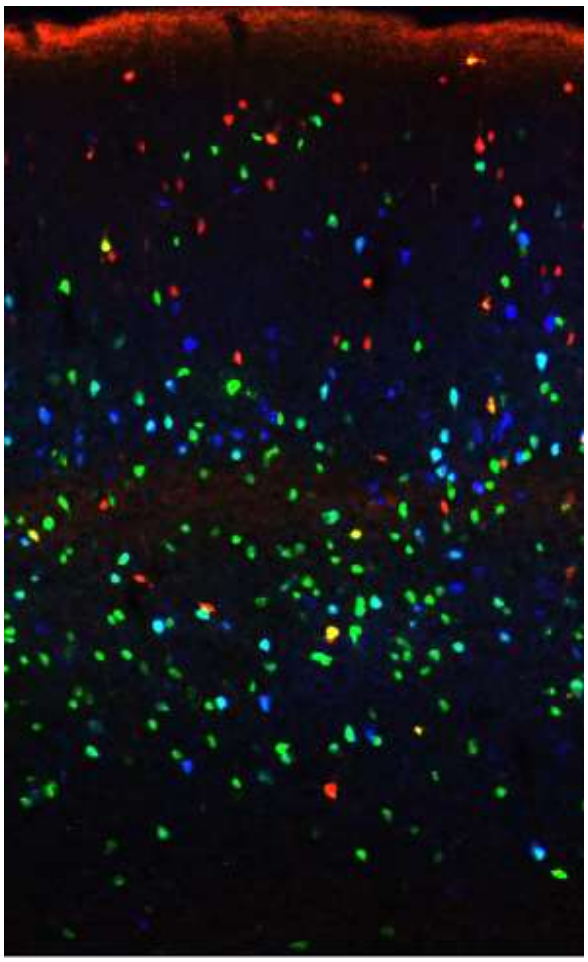

Master's Thesis

"*Cux2* in cortical interneuron development"

Theodora Velona

Supervisor: Dr Nicoletta Kessaris, WIBR, UCL

LONDON

2014

Contents

Acknowledgements

First and foremost, I would like to thank Dr Nicoletta Kessaris for giving me the opportunity to be a part of her group and complete my Master's thesis research under her supervision. I am grateful for all her advice and guidance in every step of the thesis, from the bench work to the writing process. Her exciting ideas on the experiments were a source of inspiration for my work.

My special thanks to Lorenza Magno who supervised me while I was experimenting on the synaptic measurements. She was always there to offer a well-documented answer to my scientific questions and brilliant suggestions with technical issues as well as to proofread my writings. I will always remember the fun times we had in all the special occasions for the lab.

I greatly appreciate the guidance I received from Marcio Oliveira, who initiated me in the secrets of RNA *in situ* hybridization and probe synthesis and who was there to provide detailed answers to my never-ending questions regarding science, protocols and (mostly) reagents.

Also thank you to all the people from Bill Richardson's lab, with which we shared stimulating moments of laboratory life, sunny lunch breaks in "the steps", traditional London pub afternoons and memorable lab outings in the countryside.

At this point I would like to express my gratitude to Dr Kiki Thermou and Dr Domna Karagogeos. They provided me with invaluable help and guidance in both the Erasmus process and the Graduate program. Together with Dr Kiki Sidiropoulou, they accepted me as an intern in their labs, as part of the lab rotations, and trained me to the basic principles of techniques that I used in my thesis research.

Finally, my heartfelt thanks to my family, who have always been there to support me in all my endeavours.

Summary

The *Cux2* gene encodes a homeodomain transcription factor which is strongly expressed in the vertebrate nervous system during development. It is one of the two orthologue genes of the Drosophila cut gene which patterns a specific sensory organ in the peripheral nervous system and has been implicated in the regulation of dendritic branching in the central nervous system. During mouse development *Cux2* is expressed in a group of progenitors in the subventricular zone (SVZ) of the dorsal telencephalon and in interneurons migrating from the ganglionic eminences into the pallium. In postnatal and adult animals CUX2 is localized mainly in the upper layers and sparsely in the lower layers of the cortex. Previous studies have shown that CUX2, together with CUX1 regulate the dendritic branching, spine development and synaptic formation in layers II-III of the cortex. Also, CUX2 regulates the proliferation rates in the cortical SVZ and the numbers of neurons in the upper layers of the cortex. Until now, the contribution of CUX2 in the formation of different GABAergic interneuron populations in the cortex has been poorly assessed.

In this project we investigated the possible roles of CUX2 in the development of cortical interneurons. We used a conditional knock-out mouse model (Nkx2.1-Cre; Cux2 $^{fl/\Delta}$) in which CUX2 was deleted in interneurons derived from the medial ganglionic eminence (MGE), one of the two major sources of interneurons for the cortex. Our results, deriving from immunohistochemistry and *in situ* hybridization analysis, suggest 1) an increase in PV-expressing interneuron numbers and 2) an increase in soma- and axon initial segment-targeting inhibitory synapses in the cortex. These results are supported by electrophysiological data showing raised inhibition, as a functional consequence of CUX2 deletion in cortical circuits. Finally, behavioural assessment revealed defects in sociability.

Chapter 1

Introduction

The murine cerebral cortex consists of two types of neurons: excitatory pyramidal neurons that take up ~70%-80% of the neurons, and inhibitory interneurons that constitute the remaining 20-30% of neurons (Defelipe & As 1992). Cortical interneurons feature a lot of characteristics that distinguish them from the pyramidal neurons. Most possess aspiny dendrites (Douglas & Martin 1982) and their axons branch within a cortical column, or laterally in adjacent columns, but they are never extended into subcortical areas. Different subpopulations of interneurons send their synaptic terminals onto different compartments of their target cells and they can target both pyramidal neurons and other interneurons (Markram et al. 2004).

1.1 Classification of cortical interneurons

Cortical interneurons are a very heterogeneous group. They are divided into different subtypes based on their unique morphology, electrophysiological and synaptic properties, as well as the expression of diverse biochemical markers (Kawaguchi & Kubota 1997; Gupta et al. 2000).

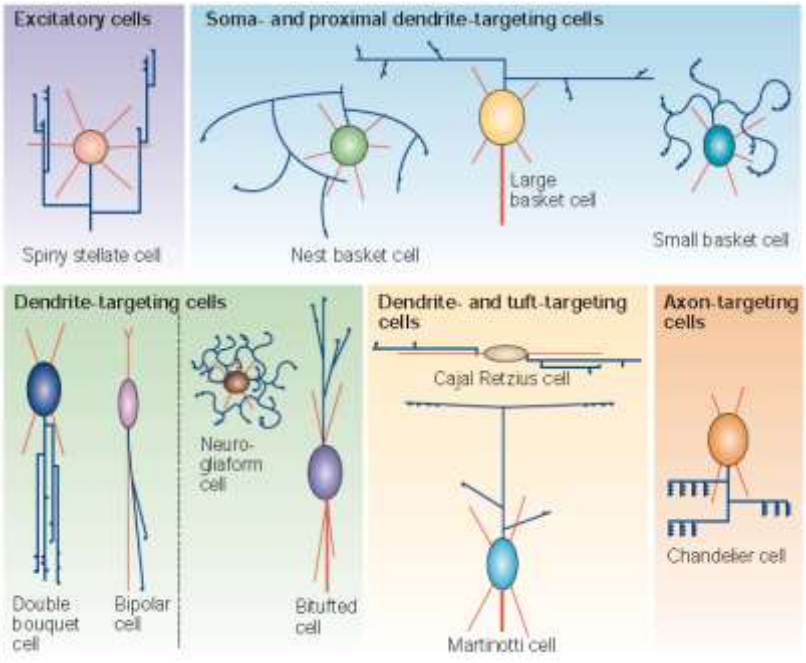

Figure 1.1 Schematic representation of the sifferent morphological types of cortical interneurons. Axons are red and dendrites are blue. Interneurons are distinguished by their target preference. (Markram et al. 2004)

The morphological characteristics of their axons reflect their functions, as they specify the cellular subdomains that they target. From this perspective, cortical interneurons can be subdivided into axon-targeting, soma and proximal

dendrite-targeting, dendrite-targeting and dendrite and tuft-targeting interneurons (Figure 1.1). The different morphological and electrophysiological subtypes of interneurons express specific combinations of calcium binding proteins, such as calbindin (CB), calretinin (CR), parvalbumin (PV) and neuropeptides, such as neuropeptide Y (NPY), vasointestinal peptide (VIP), somatostatin (SST) and cholecystokinin (CCK) (Figure 1.2). So for example, basket cells and chandelier cells, which are soma and proximal dendrite-targeting, typically express several neuropeptides, according to the subtype, and the calcium binding proteins PV and CB. On the other hand, Martinotti cells, which are tuft dendrite-targeting neurons, express always SST but never VIP (Markram et al. 2004).

1.2 The origins of cortical interneurons determine their identity

While excitatory pyramidal neurons are generated in the ventricular (VZ) and subventricular zone (SVZ) of the dorsal telencephalon (pallium) during embryogenesis, the cortical interneurons stem from the ventral telencephalon (subpallium) and follow tangential migratory pathways to reach their final positions in the cortex (Marin & Rubenstein 2003) (Faux et al. 2010). Three proliferative domains in the subpallium generate distinct populations of cortical interneurons: the medial ganglionic eminence (MGE), the caudal ganglionic eminence (CGE) and the preoptic area (POA). It is well known today that the diversity of cortical interneurons is partly defined by their embryonic origin (Kessaris et al. 2014) (Flames et al. 2007). For example, the MGE generates principally PV-expressing and SST-expressing interneurons. CR or RLN or both can be co-expressed by SST^{+ve} interneurons, which are preferentially specified within the dorsal part of the MGE, whereas PV^{+ve} interneurons are generated mainly in the ventral MGE. On the other hand, the dorsal CGE is the site of origin of SST and RLN co-expressing interneurons as well as VIP^{+ve} interneurons which may or may not co-express CR. Finally, the POA is the source of SST, RLN and PV-expressing interneurons. (Figure 1.2). Each region contributes to a different extent to the final number of interneurons with the MGE-derived population taking up more than half of the adult cortical inhibitory neurons (60%) and the CGE and POA-derived ones taking up 30% and 10% respectively.

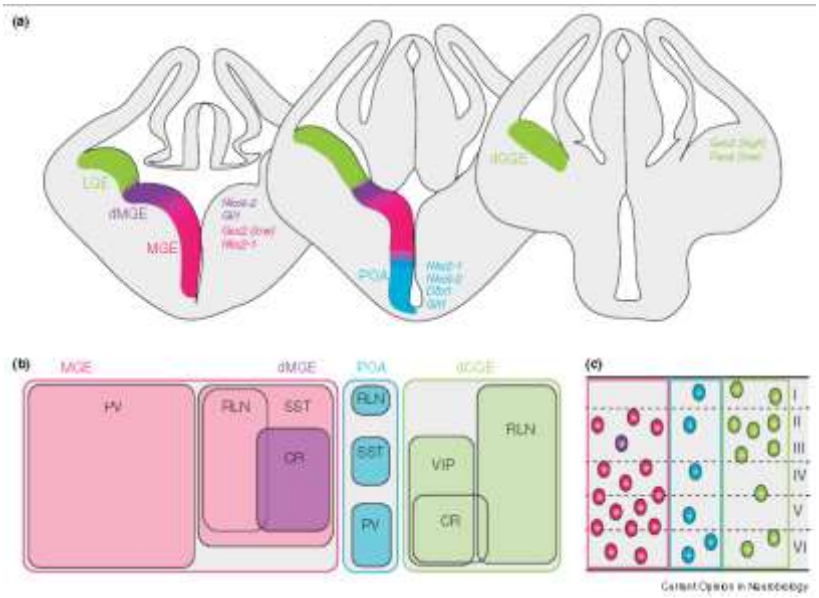

Figure 1.2 Embryonic origin and mature fates f cortical in terneurons (Kessaris et al. 2014)

This distinct differentiation potential of the different germinal zones is attributed to the expression of different combinations of transcription factors (TFs), which provide these cells with their identity (Campbell 2003). Loss-of-function (LOF) experiments for these transcription factors have shown that they can be important for cell fate commitment (molecular markers), tangential migration, radial migration inside the cortex, laminar localization and maturation of the axons and dendrites as well as their physiology. NKX2-1 is a TF expressed in MGE progenitors before the initiation of migration and it determines the specification of all cell lineages derived from this region. DLX1-2 are critical for the specification and migration of all interneurons, but, in the case of the MGE derived interneurons expressing SST NPY and CR, it acts in later stages affecting their dendritic maturation and survival. LHX6 is yet another transcription factor specific for the MGE lineage, that acts downstream of NKX2-1 and controls tangential migration, distribution in cortical layers and final differentiation of PV^{+ve} and SST^{+ve} interneurons deriving from this area. Finally, SOX6 is a downstream effector of LHX6, responsible for the correct laminar distribution and final maturation of the MGE-derived interneurons (Anastasiades & Butt 2011; Gelman et al. 2012; Kessaris et al. 2014). Other TFs have been found to act specifically in the development of interneurons from the CGE and the POA. Also studies for expression patterns have revealed TFs which are expressed in the MGE progenitors but their role in developmental aspects is under investigation. Some examples are the bHLH factor NPAS1, the bZIP MafB and the homeodomain containing ARX and CUX2 (Cobos et al. 2006).

1.3 Inhibitory interneurons form the activity of cortical networks

Inhibitory interneurons first appear in the cortex at E12-E13. GABA expression is found in the subplate, marginal zone and SVZ of the cortex until P0, when it starts to disappear and, in turn, it appears gradually in the cortical plate. This process carries on until the adult-like expression pattern of GABA is established in the cortex, at about P16 to P20 (Del Rio et al. 1992). During pre- and postnatal development, the immature GABAergic interneurons control the maturation of the activity of brain circuits and, at the same time, receive signals that affect their own maturation (Magueresse & Monyer 2013). At early stages and until the end of the first postnatal week, GABAergic transmission leads to excitation of postsynaptic cells. GABA-mediated excitation promotes the migration of interneurons and pyramidal neurons (Behar et al. 1998)(López-bendito et al. 2003; Manent et al. 2005) and when it switches to inhibition the neurons stop migrating (Bortone & Polleux 2009). This may be one of the factors controlling laminar localization of interneurons in the cortex (Miyoshi & Fishell 2011).

Immature GABAergic interneurons function as pacemakers for cortical networks and influence the properties of plasticity and synaptic wiring (Magueresse & Monyer 2013). More specifically, changes in the timing of the switch from excitatory to inhibitory effect of these neurons cause alterations in the dendritic length and level of synaptic transmission performed by pyramidal neurons (Wang & Kriegstein 2008; Wang & Kriegstein 2011)(Cancedda et al. 2007). GABA-mediated giant depolarizing potentials appear in the hippocampus at birth and reportedly strengthen the glutamatergic synapses (Mohajerani et al. 2007). This type of synchronization also exists in the cortex and could possibly serve the same cause (Allène et al. 2008). Postnatally, at about P5, GABAergic interneurons give the pace to gamma oscillations in the cortex (Yang et al. 2013). In adulthood, inhibitory interneurons organize the function of local networks of the cortex. For example, PV-expressing, soma-targeting basket cells synchronize pyramidal neuron populations in the cortex thus generating a stable rhythm of discharge. These interneurons are responsible for the generation of theta and gamma rythms in the cortex and the basic cortical processing. On the other hand, a certain group of CCK expressing interneurons control the transmission of information coming from subcortical structures, regarding the motivational, emotional and physiological state of the organism (Freund 2003; Whittington & Traub 2003). Finally, GABAergic transmission has been implicated in the plasticity shown by cortical networks after the establishment of synaptic contacts, during critical periods. Studies of the visual system have provided proof that sufficient levels of GABA release are necessary for the occurrence of the critical period. GABA could act by changing

the motility (Oray et al. 2004) or the density of spines (Mataga et al. 2004), or by changing the large-scale architecture of the cortex.

1.4 Functions and expression pattern of cut in Drosophila

CUX2 is a TF that is expressed in the MGE and is thus a candidate for controlling the development of cortical interneurons. It is the homologue of the *Drosphila* homeobox cut. CDP/Cut-like transcription factors are conserved in a wide range of multicellular organisms, including *Drosophila*, rodents, dog and human. (Iulianella et al. 2003; Andres et al. 1992) The first gene of this family to be discovered was the *cut* locus in Drosophila, where it was known to play a definitive role in the specification of the external sensory organs (Bodmer et al. 1997). A null mutation in the *cut* locus resulted in the transformation of the neurons and support cells of the external sensory (es) organs into those of chordotonal (ch), internal sensory organs of the Drosophila. Also, ubiquitous expression of the *cut* sequences resulted in the conversion of the ch organs into the es fate (Blochlinger et al. 1991). Analysis of the primary structure of the locus suggested the existence of a homeobox area and three repeated sequences that were named *cut* repeats (Brochlinger et al. 1988). The homeobox area encodes a divergent homeodomain and was suggestive of a regulatory action of the protein. This assumption was supported also by the nuclear localization of the protein.

The *cut* gene is expressed in both the cells of the external sensory organ and their precursors (Blochlinger et al. 1990). It is also expressed in other types of neurons and the cells lining malpigian tubules and can be found in all stages of development, embryo, pupa and adult. Due to its relatively late initiation of expression, i.e. just before the differentiation of es organs and not during the determination of neuronal fate, its product was considered to act as a mediator of upstream factors for the specification and/or morphogenesis of selected neuron populations. Indeed high, medium or non-detectable levels of *cut* expression in a third population of sensory neurons, called dendritic arborisation (da) neurons, were correlated with different populations of da neurons, possessing distinct dendrite morphologies. More specifically, the area of dendritic expansion and extent of dendritic branching was increasing in accordance with the level of Cut immunoreactivity and high expressing neurons were characterized by the appearance of dendritic spikes. LOF and gain-of-function experiments confirmed the hypothesis that Cut was a key transcription factor, not only for the establishment of the identity in sensory neurons, but also implicated in the morphological differentiation of their dendrites, suggesting that similar conserved functions could be found for the cut homologues in vertebrates (Brochlinger et al. 1988; Jinushi-Nakao et al. 2007). Cut seems to

exert this action in collaboration with, or by controlling the levels of the Knox transcription factor, which promotes the growth of microtubule-based dendritic branches.

1.5 Expression patterns of *Cux1* and *Cux2* in developing and adult mouse

The murine *Cux1* and *Cux2* genes are homologues of the *Drosophila Cut* gene. They are located in distinct loci (*Cutl1* and *Cutl2* respectively) on the 5th chromosome. They both contain a 183 bp homeobox domain, which is similar to the previously-described homeodomains. Indeed, four particular amino acids that exist in all homeodomain proteins, are also conserved in the CUX1 and CUX2 proteins. A histidine residue in the position 50 of the homeodomain, as well as the presence of the three cut repeats distinguished these paralogous genes from other homeobox genes and established them as members of a CUT homeobox gene family (Quaggin et al. 1997).

Cux1 is expressed in most adult tissues, such as brain, lung, heart, skeletal muscle and thymus (Valarché et al. 1993). In the developing embryo at E15, its transcripts are detected in the developing brain and specifically in the basal ganglia, neocortex, midbrain, and cerebellum, the lung, kidney and urinary tract, as well as the precartilage primordium of the limb, dorsal root ganglia, and sensory whiskers (Heuvel et al. 1996). Similarly to its *Drosophila* counterpart, it localizes to the nucleus (Andres et al. 1992).

Cux2 expression throughout development is not exclusively restricted in the neuronal system, as originally implied (Quaggin et al. 1997), but extends to several tissues. The RNA and protein can be found in developing craniofacial structures such as the cranial vault and the oral and nasal epithelia, the limb progress zone and later on the interdigital area, as well as the urogenital system. Within the nervous system they are present in both the brain and spinal cord. Very early in development (E10, E11) they occur in several regions of the neural tube, such as the roof plate, motor neuron pool, V3 interneuron progenitors and dorsal root ganglia,

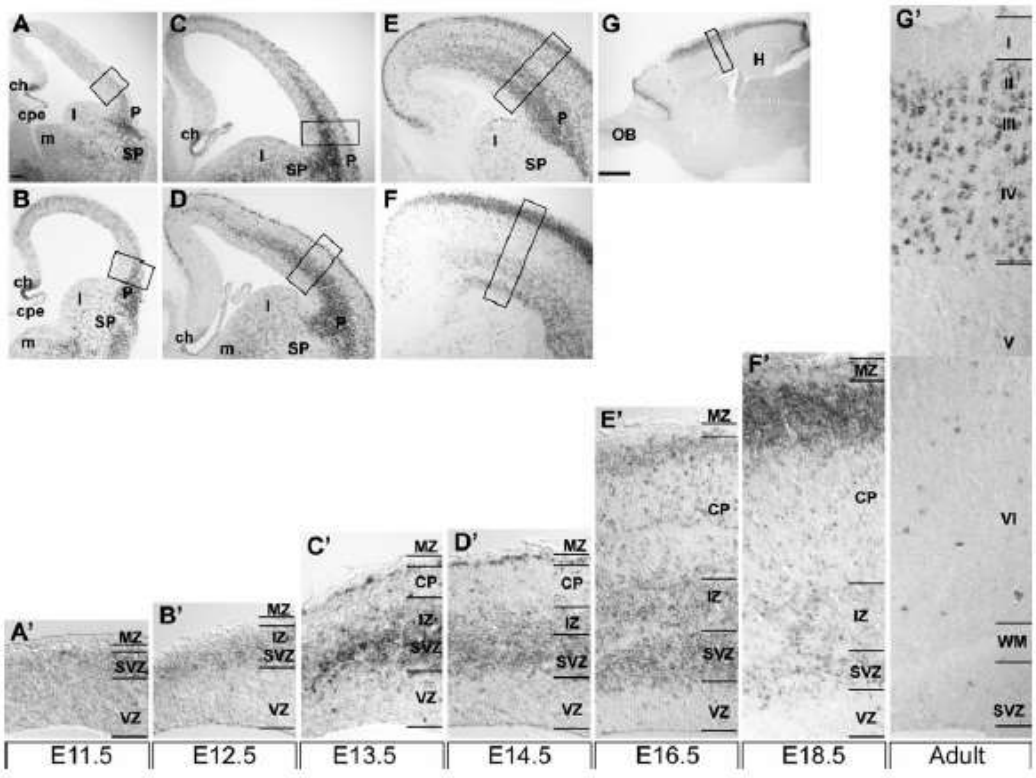

Figure 1.3 Expression of Cux2 throughout development in the mouse cortex.

where they continue to be detected until later developmental stages (Iulianella et al. 2003).

The expression pattern of *Cux2* in the developing and adult mouse brain has been described in detail (Zimmer et al. 2004) (Figure 1.3). During early stages of development (E11.5-E12.5) *Cux2* signal is located in both the subpallial and pallial areas. In the subpallium, *Cux2* is expressed by progenitor cells of the MGE and the LGE, whereas in the pallium it is increasingly expressed by progenitors residing in SVZ of the cortex, but at this stage its expression is restricted to the lateral cortex. During this period it is also found in cells of the cortical hem epithelium. Later in development (E13.5-E14.5) *Cux2* is expressed strongly at the SVZ and intermediate zone (IZ) of the lateral and medial pallium, but it can also be found in single cells of the cortical plate (CP). Strong *Cux2* expression at this timepoint can be observed at the marginal zone (MZ) where Cajal-Retzius cells reside as well as in individual interneurons migrating from the MGE and invading the dorsal telengephalon. As development proceeds (E16-E19), *Cux2* signal in the SVZ of the cortex becomes gradually weakened and in turn it becomes more intense in the superficial part of the CP, which is destined to become the upper layers (UL) of the cortex. In the postnatal and adult mouse brain *Cux2*, as *Cux1*, defines upper

layer neurons of the neocortex. Expression can also be seen in the ventrolateral and piriform cortex (Figure 1.4) (Nieto et al. 2004), as well as the globus pallidus. As opposed to *Cux1*, *Cux2* is also present in isolated cells of the cortical deep layers (DL) and cingulate cortex in a pattern that is reminiscent of cortical interneurons. Similarly to *Cux1*, we observe *Cux2* expression in neurons of the claustrum and endopiriform nucleus.

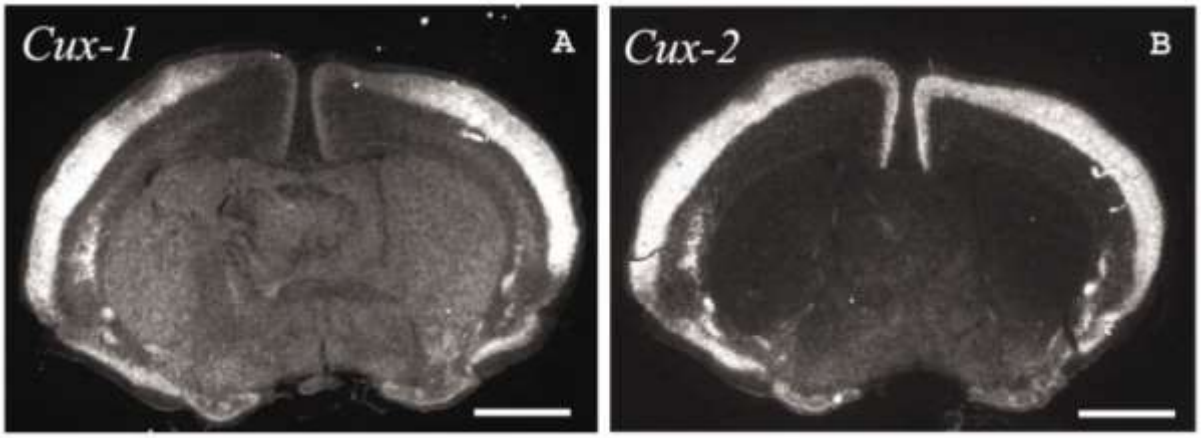

Figure 1.4 Expression patterns of Cux1 and Cux2 in the adult cortex. (Nieto et al. 2004)

1.6 Roles of CUX2 in development of neuronal populations

As described in the previous paragraph, *Cux2* is expressed in the intermediate progenitors of the cortex giving rise to post-mitotic upper layer cortical pyramidal neurons. Other tissues undergoing intense proliferation in the developing mouse embryo (such as the limb bud progress zones and the urogenital tissues) also express *Cux2* suggesting a role in this process. Indeed, CUX-2 has been found to control cortical upper layer neuron numbers (Cubelos et al. 2008). Analysis of markers labelling cell-cycle stages, such as BrdU, Ki67 and pH3 suggested that this effect is achieved through the blocking of intermediate precursor proliferation in the SVZ of the cortex and particularly by limiting the number of times these precursors re-enter the cell cycle. This is supported by another study showing that radial-glia cells that express CUX2 during neurogenesis in the cortex are more prone to proliferation than the non-expressing ones. CUX2 delays their cell cycle exit and as a result their progeny are born later and occupy the upper layers of the cortex, forming the typical inside-out arrangement of cortical pyramidal neurons (Franco et al. 2012).

A direct demonstration that CUX2 regulates cell cycle progression in neuronal progenitors was also performed in the developing murine spinal cord (Iulianella et al. 2008a). More specifically, this study

showed that CUX2 is important for the formation and/or maintenance of progenitors in the VZ of the spinal cord and exerts its action through the activation of the bHLH factor NeuroD and the subsequent proper G2/M transition. Later in development, correct dosage of CUX2 in the ventral intermediate zone of the spinal cord is required for the differentiation and specification of interneuron populations. This is mediated by the expression of the p27Kip1 gene which promotes the properly timed cell-cycle exit of nascent neurons in this area. CUX2 targets directly the p27Kip1 gene by being present in activating complexes binding its native promoter. Hence, it seems to be important for not only cell cycle progression and proliferation but also for differentiation of interneuron populations, at the expense of motor neurons. These interneurons reside both in the dI3-dI6 layers of the dorsal spinal cord and the commissural interneurons that are progeny of dI1-dI2 interneuron subgoups (Iulianella et al. 2008b). CUX2 is exerting this effect by acting as a downstream effector of the Notch signalling pathway (Iulianella et al. 2009).

CUX2 regulates neurogenesis in the olfactory epithelium of chicks and mice. At low levels of expression it promotes maintenance of the already established neuronal stem cell pool. On the other hand, higher levels of *Cux2* occur as a result of bone morphogenic protein (BMP) signalling and inhibit neurogenesis while exerting negative effect on Notch signalling.

In addition to proliferating cells, CUX1 as well as CUX2 have been shown to regulate important aspects of postmitotic neuron differentiation, such as dendritogenesis and synaptogenesis (Cubelos et al. 2010). More specifically, CUX1 and CUX2 positively regulate the length and degree of branching of upper layer neuron dendrites. They also exert control on spine density and maturation in layer II-II neurons. This is possible either directly, by repressing the expression of X-linked lymphocyte regulated (Xlr) 4b and Xlr3b, two genes that are believed to be chromatin remodelling, or indirectly by downregulating the expression of NMDAR2B and PSD95 post-synaptic proteins. These actions are cell-autonomous and they are reminiscent of the functions of the Drosophila *Cut* gene in the dendritic branching in the PNS.

Apart from spinal cord interneurons and cortical upper layer neurons, *Cux* genes have also been implicated in the development of cortical interneurons as mutants lacking both *Cux1* and *Cux2* show severe reduction of Reelin^{+ve} interneurons in layers II-VI of the cortex (Cubelos et al. 2008). However, the precise function of *Cux* genes in cortical interneuron lineages has not been investigated.

Aim of the study

This study aims to investigate the function of CUX2 in the development of cortical GABAergic interneurons. We made use of a conditional knockout mouse in which *Cux2* was deleted from the MGE neuroepithelium and MGE-derived cortical interneurons. We examined the consequences of CUX2 loss on cortical interneuron numbers, connectivity, inhibitory transmission and mouse behaviour.

Chapter 2

Materials and Methods

2.1 Transgenic animals

To investigate the role of CUX2 in the development of MGE-derived cortical interneurons we used BAC transgenic mice expressing Cre recombinase under control of the *Nkx2-1* gene (Nkx2-1-Cre^{Tg}) (Kessaris et al, 2006) together with a mouse carrying a conditional mutant allele for *Cux2 (Cux2$^{fl/fl}$)* (provided by F. Guillemot). The *Cux2* gene contains 23 exons and encodes 3 DNA-binding cut domains and a homeodomain. The *Cux2* conditional mouse line contains one loxP site between exons 20 and 21 and a second loxP site downstream of the polyadenylation site in exon 23. Cre excision results in deletion of the cut domains 2 and 3, the homeodomain as well as the endogenous transcriptional stop codon and polyadenylation site. As expression of *Nkx2-1* is restricted to MGE precursors and excluded from cortical precursors where Cux2 is also expressed, deletion of CUX2 using Nkx2-1-Cre is specific to subcortical regions. (Fogarty 2007). These include the MGE (with the exception of a small region in the dMGE), the POA, and the posterior part of the ventral septum (Kesssaris et al, 2006). The neomycin resistance cassette used for ES cell gene targeting during the generation of the *Cux2* conditional allele had been removed by FLP excision prior to the mice being used for experiments. To achieve more efficient recombination in our experiments, we generated a germline loss-of-function (LOF) allele for *Cux2* by crossing the conditional *Cux2* mice to a mouse expressing Cre in the germline. We refer to this germline-deleted allele as Cux2$^{\Delta}$. To visualise cells where deletion of the gene has taken place we also made use of a mouse line that expresses a YFP reporter gene upon Cre recombination (R26R-YFP$^{KI/KI}$) (Srinivas et al, 2001).

To obtain mutant and control animals for our studies we mated hemizygous Nkx2-1-Cre^{Tg}; Cux2$^{+/\Delta}$ mice with Cux2$^{fl/fl}$;R26R-YFP$^{KI/KI}$ mice. Nkx2-1-Cre^{Tg};Cux2$^{fl/\Delta}$ mice were used as conditional mutants (cKO) and the rest of the genotypes were used as controls, depending on whether GFP expression was needed for the study.

2.2 Tissue preparation

2.2.1 Embryonic tissue

The morning of the vaginal plug was considered embryonic day (E) 0.5. At the appropriate embryonic day the mother was sacrificed and the embryos were extracted and kept in Phosphate Buffer Saline (PBS) treated with diethyl pyrocarbonate (DEPC, Sigma, used in 1:1000), at 4ºC. The brains were dissected and kept overnight in 4% (w/v) Paraformaldehyde (PFA) for fixation. Subsequently they were immersed in DEPC treated sucrose 4% (w/v) in PBS and left overnight for cryoprotection. Finally, they were embedded in moulds filled with optimal cutting temperature (OCT) compound (Tissue Tek; Raymond Lamb Ltd Medical Supplies) and frozen by immersion in methanol over dry ice. The samples were kept at -80ºC.

2.2.2 Adult tissue

The morning when a litter birth was observed, was set as postnatal day (P) 0.5. Adult mice were perfused transcardially with DEPC-treated PBS and 4% (w/v) PFA. The brains were dissected out and for better penetration of the fixative they were cut into four coronal slices of 2mm thickness using a brain slicer. The slices were processed for fixation as described above for the embryonic brains.

2.3 Histological stainings

2.3.1 In Situ Probe Synthesis

2.3.1.1 DNA digestion and extraction

One of the probes for detecting the deleted region of *Cux2* was synthesized during this study, while the RNA probes for WT *Cux2*, *Cux1* and *Lhx6* had already been made and stored in the freezer as aliquots. 2.5µg of maxiprep plasmid DNA was digested overnight at 37ºC in a digestion buffer containing 1µL of a suitable restriction enzyme (Not1, New England Biolabs), restriction enzyme buffer 10% (v/v) and BSA (10µL, Sigma). 2.5 µL of the digested template were kept at -20ºC for later use. 2.5µL of 20% SDS (Sigma) and 2µL of Proteinase K (PK) were added the following day and the digestion tube was incubated for 15 minutes at 55ºC. Following this, two steps of pheno-chloroform extraction were performed. In the first step a volume of phenol (Sigma) equal to the

volume of the starting solution was added, the solution was centrifuged at 13.4 rpm for 2 min and the supernatant was kept. The same process was repeated adding chlorophorm (BDH) to the solution. The extraction was completed with a precipitation step, in 100% ethanol (VWR) and sodium acetate (Sigma). Sodium Citrate was added at 10% of the solution volume and 100% ethanol was added at twice the volume of the solution. The final mixture was incubated on dry ice for 20 min, then spun at 13.4 rpm for 10 min. All liquid was removed and the DNA pellet was reconstituted in 50 μL of distilled water. 2.5μL of the template were run on a 1% agarose gel next to 5μL of digested but un-extracted DNA that had been kept previously, in order to estimate the quantity of the extracted DNA.

2.3.1.2 Probe synthesis reaction

A 25μL template reaction was set up, containing 2 μL of 5x transcription buffer (Promega), 3μL of DTT (Promega), 0.4μL of RNAse inhibitor (Promega), 1 μL of DIG nucleotide labelling mix (Roche), 0.2 μL of Sp6 polymerase enzyme (Promega), 3.4 μL of the DNA template and 2μL of MilliQ water. The mixture was incubated at 37ºC for 2 hours and 75μL of DEPC treated water was added afterwards. 5μL of the reaction solution was run on a 1% gel in order to confirm the synthesis of the RNA probe. The probe was aliquoted and stored at -80ºC.

2.3.2 In situ hybridization on embryonic sections

Sections of the frozen tissue, 15 μm in thickness, were collected on Superfrost Plus slides (VWR International) on a Bright OTF5000 cryostat and left to dry at room temperature for 1 hour. The probes were diluted at 1:1000 in hybridization buffer. This buffer consists of 50% formamide, 100mg/ml dextran sulphate, 1mg/ml tRNA, 1x Denhardt's solution (50x stock, 1% Ficoll 400, 1% polyvinylpyrrolidone, 1% bovine serum albumin). The solution was incubated for 5-10 min for denaturation and applied onto the slides. Coverslips that had been baked at 200ºC were placed on top of the probe to minimise evaporation. A hybridization chamber was prepared, which was composed of two glass trays containing two pieces of Whatman paper dipped in washing buffer for in situ (50% v/v formamide and 1x SSC) and a piece of Parafilm, on top of which were placed the slides. The chamber was placed in an oven, for overnight incubation at 65ºC, so that hybridization of the probe takes place. All the reagents used in this step were DEPC treated, in order to inactivate the RNAases.

After the hybridization step, the coverslips were removed either by inclination of the slide or by dipping the slides in a Coplin jar filled with post-hybridization Washing Solution, which was pre-heated at 65ºC. The solution was made of 50% formamide, 1x SSC and 1.1% Tween-20). Two additional 30 minute washes in this buffer at 65ºC followed. Subsequently the sections were rinsed in MABT, for 2X 30 minutes at room temperature. Afterwards, the sections were blocked for 1h at room temperature, using an in situ blocking buffer (2% w/v blocking reagent (Roche), 20% heat inactivated sheep serum in 1.2x MABT). A primary anti-DIG antibody conjugated with Alcaline Phosphatase (AP) was applied after the blocking step. The antibody was diluted in the blocking buffer described above at 1:1500 and the sections were incubated overnight at 4ºC.

The excess of the anti-DIG antibody was removed by washing for 2x30 minutes in MABT. A pre-staining buffer (0.1M Nacl, 50mM MgCl2, 0.1M Tris pH9.5, 0.01% Tween-20) was prepared and used for a brief washing step, in order to condition the sections for the following stain step. A staining buffer was made using 20 ml of the pre-staining buffer, 1ml of 1M $MgCl_2$ solution, 87µl of NBT (4-nitro blue tetrazolium chloride, Roche, 1g in 7ml dimethyl formamide and 3ml distilled water), 67µl BCIP (5-Bromo-4-chloro-3-indolyl phosphate, Roche, 1g in 7ml dimethyl formamide) and 20 ml PVA (polyvinyl alcohol, 10% w/v in pre-staining buffer without $MgCl_2$). The sections were incubated in this buffer until blue signal could be seen clearly. The reaction was stopped by immersion of the slides in tap water. The sections were then dehydrated by immersion in IMS solutions of gradually increasing concentration (65%, 80% and 95% for 1 minute each), then in pure ethanol (for 1minute and after in a second jar for 2minutes) and finally in pure xylene (2x2 minutes). The dehydrated slides were coverslipped using DPX mountant (Fluka).

2.3.3 In situ hybridization on postnatal and adult sections

Coronal sections of 30µm thickness were collected in the cryostat using a brush and placed in wells of 24 well plates, containing DEPC treated PBS. The sections were carefully mounted on Superfrost slides using a fine and a coarse brush and left to dry at room temperature for at least 1hr. In situ hybridization was then carried out as described for the embryonic tissue.

2.4 **Immunohistochemistry**

2.4.1 On cryosections

Fixed and frozen slices of brain of 2mm thickness were further sectioned on a cryostat to obtain sections of 30 μM thickness. The sections were then collected using a thick brush in PBS filled wells of 15.6 mm diameter (24 well plate). The entire staining process took place inside the wells. Firstly, the PBS was removed. Blocking buffer (PBS, 0.1% Triton X-100, 10% heat-inactivated sheep serum) was added in each well and the sections were left at room temperature for 1hr, to block non specific binding. Primary antibodies were diluted in blocking buffer (dilutions indicated in Table 2.1) and 300 ml of the appropriate antibody mixture was added in each well after removing the blocking solution. The well plate was then transferred on top of a shaker in a 4ºC cold room, for overnight incubation.

After the primary antibody incubation the sections were washed for 3x20 minutes in PBST (PBS with 0.1% Triton X-100). The appropriate Alexa Fluor-conjugated antibodies were diluted in the blocking buffer for immunohistochemistry at 1:1000 and 400ml of secondary antibody solution was added in each well after suctioning away the PBST from the last wash. Hoechst (10 mg/ml stock) was included in the solution, diluted at 1:1000. The sections were incubated shaking in the dark at room temperature for 1.5 hours and then washed for 3x20 minutes in PBS. The sections were spread on top of Superfrost Plus slides and coverslipped using Fluorescent Mounting Medium (Dako). They were kept at 4ºC in the dark.

2.4.2 On vibratome sections

For the measurement of total synapses immunohistochemistry was performed on vibratome sections from fresh tissue. Mice were decapitated, and the brain was quickly dissected, and immersed into artificial CSF (NaCl 150mM, KCl 3mM, $CaCl_2$ 2mM, NaH_2PO_4 1.25 mM, $NaHCO_3$ 26mM, D-glucose 10mM in milliQ water, pH7) in 24 well plates. The sections were then fixed in 4% PFA and 4% sucrose at room temperature for 1 hour without shaking. After 3x20 minute washes in PBS, blocking buffer (donkey serum 10%, 0.2% Triton-X 100 in PBS) was added into the wells. After a 4 hours blocking step, the appropriate primary antibodies (dilutions shown in Table 2.1) were added to the wells and the sections were left overnight shaking at 4ºC. On the second day the sections were washed 3 times with PBS over 2 hours, and the appropriate secondary antibodies, diluted at 1:600, and Hoechst diluted at 1:1000 in blocking buffer were added for 2 hours. Three more washes in PBS

over 2 hours followed and the sections were mounted on Superfrost slides, using fluoromount-G as mounting medium and coverslipped. The slides were kept in the dark at 4ºC.

Antibody specificity	Raised in	Dilution	Company
anti-Calretinin	rabbit	1:1000	Swant
anti-Parvalbumin	mouse	1:1000	Chemicon
anti-Somatostatin	rabbit	1:200	Peninsula Labs
anti-NPY	rabbit	1:1000	RayBiotech
anti-VGAT	guinea pig	1:500	Synaptic Systems
anti-VG1	guinea pig	1:1000	Synaptic Systems
anti-Gephyrin	mouse	1:500	Synaptic Systems
anti-PSD95	rabbit	1:500	Millipore
anti-NeuN	mouse	1:1000	Millipore
anti-pIkBa	rabbit	1:1000	Cell Signlling Technology
anti-GFP	rat	1:1000	Nacalai tesque

Table 2.1 List of antibodies used for immunohistochemistry

2.5 Imaging and Quantification

2.5.1 Interneurons

Interneuron marker staining was imaged using a standard fluorescent microscope (Zeiss AXIOPLAN). Images of the entire dorso-ventral extent of the cortex were obtained under a 10x magnification lens. Images were taken from the motor cortex (primary motor area) and somatosensory cortex (primary somatosensory area-upper limb and barrel cortex). For each area, two

sections were imaged from each hemisphere and for each animal. The sections were derived along the rostro-caudal extent between the following levels: rostrally where the corpus callosum of the two hemispheres is connected and caudally finishing slightly before the hippocampus. Images spanning the dorso-ventral extent of the cortex were stitched together with Microsoft ICE. Contrast was enhanced in Photoshop CS3 extended (Adobe Systems) and a rectangular frame of a defined width was used for defining the area of quantification. The thickness of this frame was adjusted depending on the thickness of the cortex as it extended from the pial surface to the corpus callosum. The frame was divided into 10 equal bins along the dorso-ventral axis and cells in each bin were counted. The number of cells for each mouse represented the mean of the counted interneurons in the four hemispheres. The results are depicted as mean within animals and the error bars represent the standard error of the mean (S.E.M.). At least three animals per genotype were used and statistical significance was calculated using Student t-test and non-parametric tests where necessary.

2.5.2 Synapses

Quantification of synaptic markers was carried out using Confocal images acquired on a Perkin-Elmer spinning disc microscope or Leica SPE2. Serial square planes of 0.114μm width and 0.114 μm length were obtained for each colour channel using a 63x magnification. The distance between the planes was 0.42 μm. One section per animal was used to obtain four confocal stacks, each of which contained more than ten nuclei or axon initial segments. We obtained 12 planes per stack for quanification of synapses onto AIS and 26 planes per stack for the perisomatic synapses. The area we chose for this quantification was the most dorsal part of layers II-III of the somatosensory cortex (barrel field).

Images were analyzed using the Perkin Elmer Volocity Software. In order to count the number of total synapses, as well as the number of VGAT puncta per AIS and per cell body, three respective protocols were created (Figures 2.1, 2.2, 2.3), combining the appropriate measurement protocol tasks provided by the program for this purpose. The first one quantified the apposition of pre- and post-synaptic markers, indicating the total number of excitatory and inhibitory synapses in an image. The other two protocols counted the number of items (VGAT-channel 2) that were in contact with each item in channel 1 (pIkBa/AIS or NeuN/soma).

Protocol 1: VGAT-Gephrin (for GABAergic synapses), Vglut-PSD95 (for glutamatergic synapses).

This protocol was designed to detect the apposition between the VGAT and the Gephyrin staining puncta (Fig 2.1). This was achieved by defining the two stainings as two different populations. The puncta of the first population (VGAT) could be found in channel 1 (far red, 647 nm), their lowest intensity was determined at 20% of saturation and their size could range from 0.1 μm^3 to 3 μm^3. A task for separating objects was added to the protocol, in order to distinguish two different puncta. The object size index for this separation was set at 0.3 μm^3. The same task combination was used to determine the Gephyrin puncta. In this case the puncta could be found in channel 2 (red, 568 nm) and the intensity threshold was set at 15% of saturation. These two populations were used to create a third population of objects which excluded any object of VGAT population that did not touch any Gephyrin object , thus labelling the appositions between the two markers, that signal the existence of a synapse.

A

Figure 2.1 Quantification of total GABAergic synapses. A) Protocol 1, used for measuring the total number of GABAergic or glutamatergic synapses in an image. The colours of the different task units indicate the colour by which each group of objects are labelled.

(following page) B) Gephyrin puncta labelled by the second part of the protocol. C) VGAT puncta labelled by the first part of the protocol. D) Apposition of the two populations labelled by the third part of the protocol. White arrows show examples of the double laballing. Scale bars indicate 6um.

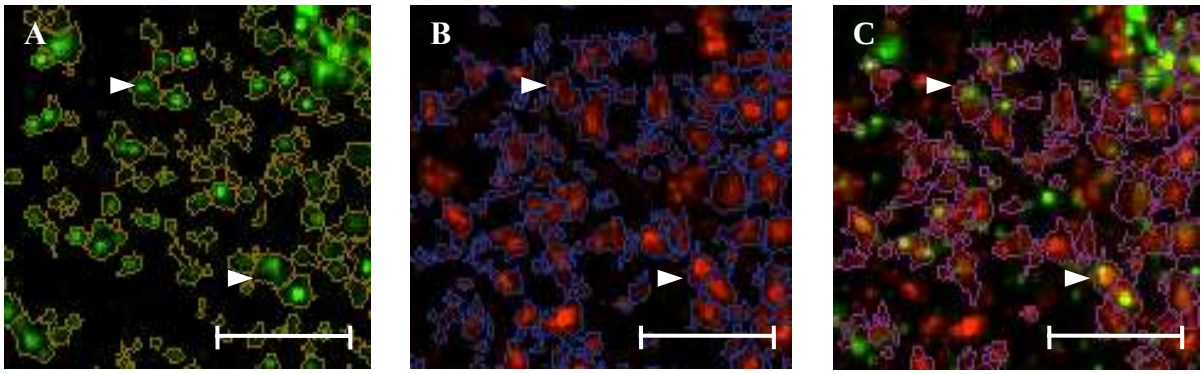

Protocols 2 and 3: Vgat-NeuN and VGAT-pIkBa

Protocols 2 and 3 share the same principle, which is to create two different populations . The first population labelled is the soma or axon initial segment and the second is the VGAT puncta. The objects of the first population are divided into groups according to which object of the first population they are in contact with. The puncta that are not touching any AIS or cell body are not taken into account. (Fig. 2.2, 2.3). The parameters for the VGAT population were established by preliminary trials in test images and the intensity threshold was adjusted accordingly (6% of saturation for AIS and 10% for soma). The size limits were set between 0.5 μm^3 and 6 μm^3. The difference between these two protocols and the VGAT-Gephyrin protocol was due to the different types of microscopes used. For the former we used the Leica SPE6 Confocal, whereas for the latter we used the Perkin Elmer spinning disc microscope. However, as suggested by the previous bibliography (Kubota 2000), these alterations do not fall far from the naturally occurring range of volume for GABAergic synaptic boutons (Fig. 2.4). The NeuN population could be found in channel 1 (red, 568 nm), only objects bigger then 200 μm^3 were taken into account and a separating object task and filling holes in objects task were added. On the other hand, as AIS we labelled objects found in channel 1 (red 568) and only objects bigger than 17 μm^3 were counted. Finally, a task for compartmentalization was added in the protocol, by which the VGAT puncta were divided per cell body or per AIS, and measurements were performed on this basis. This means that the number of puncta in each compartment (cell body or AIS) could be automatically assessed by the program and the results were arranged in excel sheets. We dictated, through the task menu, that the puncta should be overlapping with the AIS, which means that they should be touching, in order to be considered part of the compartment.

Figure 2.2: Quantification of perisomatic VGAT puncta. A) Protocol 2, used for measuring the number of GABAergic synapses that touch a cell body. B), C) Example (one plane of the z-stack) of the perisomatic puncta labelling. Red staining: NeuN. Green staining: VGAT. The VGAT puncta are labelled by the first part of the protocol. The cell bodies are labelled by the second part of the protocol. The third part compartmentalizes the first population according to the objects of the second. White arrows show examples of VGAT puncta. Scale bar: 12.00 µm

Figure 2.3: Quantification of AIS targeting VGAT puncta. A) Protocol 3, used for measuring the number of GABAergic synapses that touch an axon initial segment. B) Example (one plane of the z-stack) of the AIS targetting puncta labelling. Red staining: pIkBα Green staining: VGAT. The VGAT puncta are labelled by the first part of the protocol. The cell bodies are labelled by the second part of the protocol. The third part compartmentalizes the first population according to the objects of the second. Scale bar: 12.00. The objects that do not resemble axon initial segments are not taken into account in the statistical analysis.

Table 2. Sizes of synaptic structures of FS and LTS cells

Cell type	Postsynaptic target	Bouton volume Mean ± SD (μm^3)	n
FS	Dendrite	0.262 ± 0.126 (0.103 – 0.722)	27
	Soma	0.281 ± 0.09 (0.161 – 0.371)	11
LTS	Dendrite	0.191 ± 0.125 (0.043 – 0.523)	27
	Soma	1.116	1

Ranges are in parentheses.

Figure 2.4 Table summarizing the volumes of presynaptic boutons measured in three-dimensional reconstructions from electron microscopic images of intracellularly stained GABAergic axon terminals (Kubota Y. and Kawaguchi Y., 1999)

2.6 Mouse behaviour-Sociability test

To measure aspects of social behaviour in the conditional knockout mice, Crawley's sociability and preference for social novelty test was used. Crawley's test is performed in a rectangular box divided into three chambers (Fig 2.5). The walls dividing the chambers contain doors in the middle, which permit access to each chamber. A wire cage, in a cup-like form, big enough to fit a mouse, is placed in the middle of each of the two side chambers. This cage has a removable lid and the vertical wires are close enough to each other to restrict a mouse, but far enough to allow indirect contact with the tested mouse, which is outside. The test includes a period of habituation and the session for sociability assessment. During the habituation, the doors of the side chambers are closed. The mouse is placed in the centre of the middle chamber and left there to become familiarized with the environment for 5 minutes. In the session for sociability assessment a control mouse is placed in one of the cages. The tested animal is placed in the middle of the central chamber and the doors open allowing access to the side compartments. This session lasts for 10 minutes, during which the mouse is monitored and specific parameters are scored, with the aim to assess the sociability (social affiliation aspect) of the tested mouse. The parameters scored in this study were the number and duration of contacts with each cage and the duration of entries in each compartment.

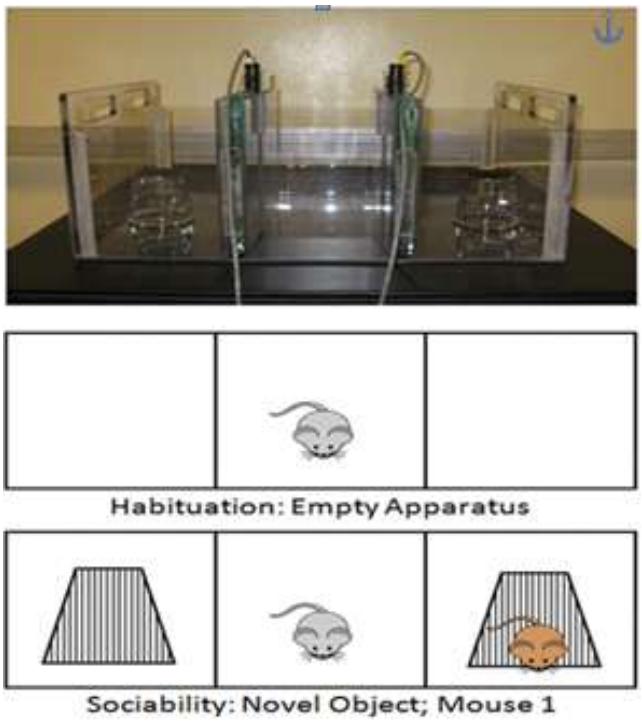

Figure 2.5 Set-up for Crawley's sociability test. Top: Image of the three-chamber box with the empty wire cages. Bottom: Cartoon showing the arrangements followed during habituation and during the session for sociability assessment.

Chapter 3

Results

3.1 Conditional deletion of *Cux2* in the MGE: normal migration of interneurons to the cortex at embryonic stages

In order to confirm the deletion of *Cux2* exons 21-23 in the MGE of conditional mutant embryos we performed RNA *in situ* hybridization at E13.5 using an RNA probe that detects the predicted deleted region of the mRNA. In WT embryos expression of *Cux2* can be seen in the subventricular zones (SVZ) of the MGE and the developing cortex (arrowheads). In Nkx2-1-Cre^{Tg};Cux2$^{fl/\Delta}$ conditional mutants (hereafter referred to as conditional knockout mice or cKO or conditional mutants) the signal in the SVZ of the MGE was lost, as expected. In contrast, the *Cux2* mRNA signal in the SVZ of the cortex was detected albeit at lower intensity (Figure 3.1). The intensity difference observed in the SVZ of the cortex is due to the fact that the mutants contain one allele of *Cux2* that is deleted in the germline (Cux2$^{\Delta}$) whereas control embryos express *Cux2* from both intact alleles. This approach had been adopted for more efficient deletion of *Cux2* and based on previous observations that mice heterozygous for *Cux2* are indistinguishable from controls (Cubelos 2008).

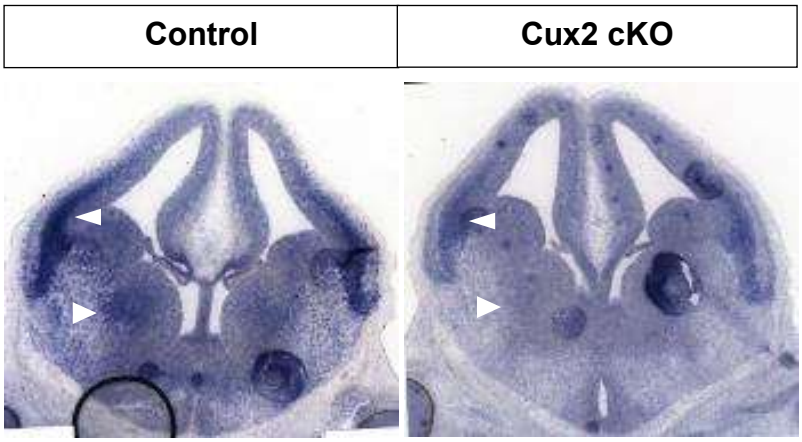

Figure 3.1: Confirmation of the deletion of the *Cux2* exons 21-23 in the MGE of embryos at E13.5. RNA *in situ* hybridization using a probe detecting the deleted region of the gene. Arrowheads show the expression of *Cux2* in the SVZ of the MGE and developing cortex in control embryos and the loss of signal in the SVZ of the MGE in the conditional mutants.

3.2 Normal migration of MGE-derived interneurons in *Cux2* conditional mutant embryos

As *Cux2* is expressed in the SVZ of the MGE and a deletion could potentially impact on the early development of these cells as they exit the ventricular zone, we examined conditional mutant embryos at E13.5 for expression of *Lhx6*, the definitive marker and lineage tracer of

MGE-derived interneurons in the telencephalon (Fogarty 2007). Expression of *Lhx6* in the subcortical telencephalon was normal in *Cux2* conditional mutants and in the cortex the two expected migration streams of MGE-derived cortical interneurons were clearly delineated (arrows) (Figure 3.2). This suggested that migration of these cells to the cortex was unaffected in the absence of *Cux2*. Quantification of the numbers of interneurons and the extent of their migration (how far the interneurons had migrated into the cortex) had not been carried out due to unavailability of embryos at the right age. Such an analysis would have indicated whether there are defects in the generation of these cells during embryogenesis.

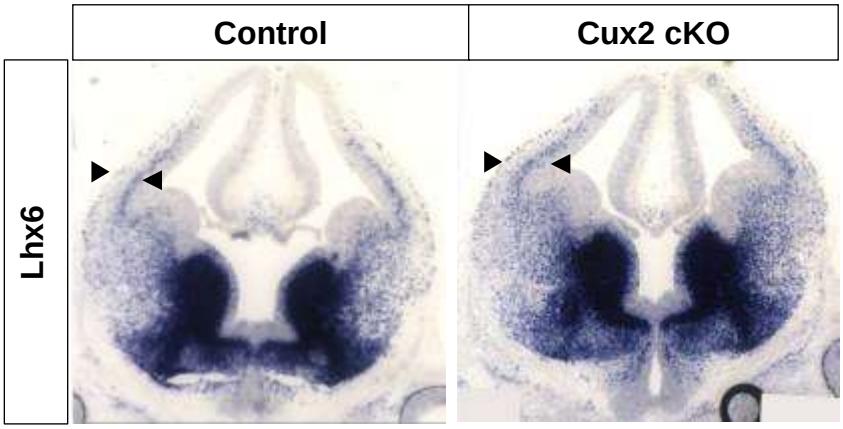

Figure 3.2. MGE derived interneurons migrate normally in *Cux2* cKO embryos. *In situ* hybridization for *Lhx6* labels post-mitotic MGE derived interneurons at E13.5. Arrowheads show the two migration streams of MGE-derived interneurons, in the preplate (dorsally) and the intermediate zone (ventrally).

3.3 Increased numbers of PV- and SST-expressing interneurons in *Cux2* conditional mutant mice at P19

One of the two major defects observed in the cortex of germline *Cux2* mutants is the presence of supernumerous upper layer cortical pyramidal neurons due to defective cell cycle exit of *Cux2*-expressing cortical SVZ precursors. Any possible defects in the numbers of cortical interneurons in Germline mutants would have been masked by the enlarged cortex. To determine therefore whether *Cux2* in the subcortical SVZ has a similar role, we examined cortical interneuron numbers in our conditional MGE-deleted *Cux2* mutants at P19 using immunohistochemistry for Parvalbumin (PV) and Somatostatin (SST) (the two major interneuron subtypes that originate in the MGE) as well as Neuropeptide Y (NPY), calretinin (CR) and Vasointestinal Peptide (VIP) (which detect interneurons originating mainly outside the MGE). We found a 25% rise in the number of PV neurons (n=5, **p=0.02**) in the somatosensory cortex of cKO mice (Figure 3.3A). A tendency for an increase in PV interneurons was also observed in the motor cortex but this was not statistically significant (n=5, p= 0.28) (Figure 3.3B). A slight increase in the number of SST-expressing interneurons

was observed in the somatosensory and motor cortices of cKO mice compared to controls at P19 (Figure 3.3 A-B), but this was not statistically significant (somatosensory: n=5, p= 0.07, motor: n=5, p=0.1) . Interneurons expressing NPY, CR and VIP failed to show changes at both stages examined and in both cortical areas, consistent with a mixed or non-MGE origin of these cells (Figure 3.3A-B). We also quantified the numbers of cortical interneurons in older animals (P60) using the same approach. We could not detect any differences between control and conditional mutant animals at this age (Figure 3.3C-D). Our results indicated that *Cux2* expression is required for establishment of normal interneuron numbers at P19. However, at later stages homeostatic mechanisms may operate to correct these errors.

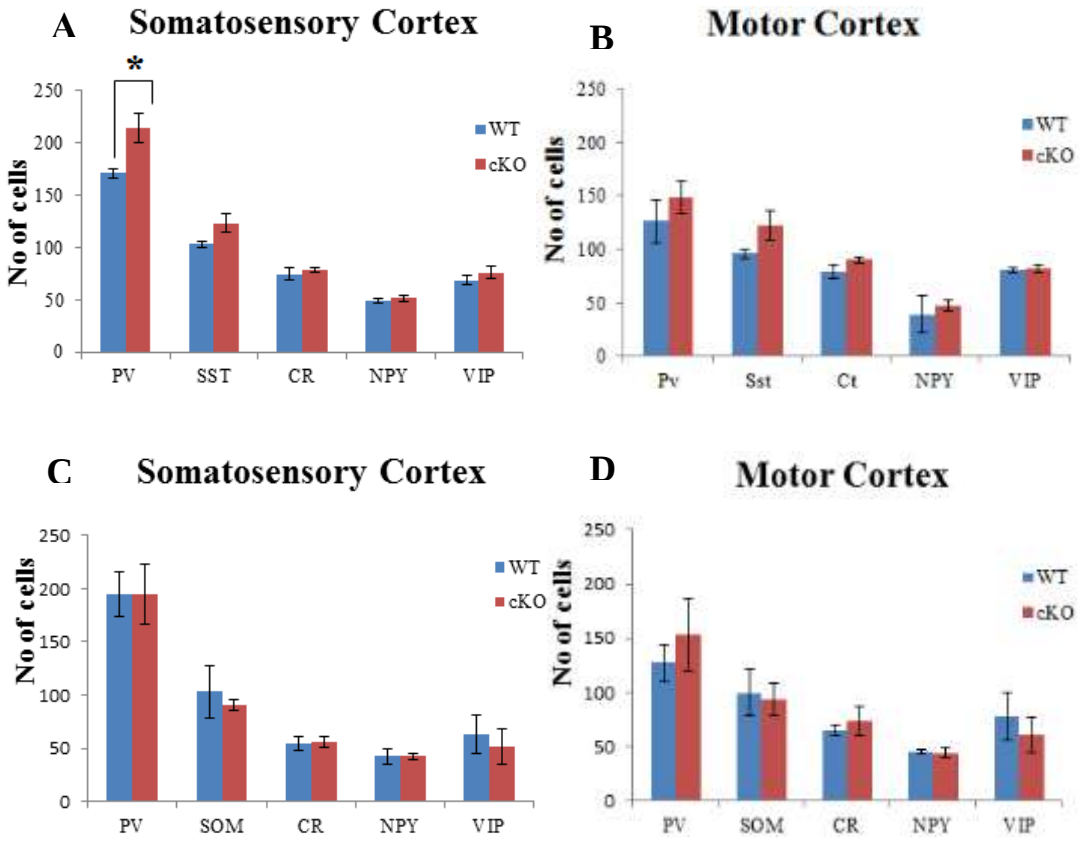

Figure 3.3 The number of PV cells is raised in the cortex of Cux2 conditional knockout animals at P19. Quantification of the cells counted in a cortical area of specified width. A), B) Cell numbers at P19. C), D) Cell numbers at P60.

The increase in the number of MGE-derived interneurons in the cortex prompted us to examine the distribution of these cells in more detail. The aim was to determine whether additional interneurons are concentrated in specific layers or are distributed widely within the cortex. For this we subdivided the cortex into 10 equal bins and quantified the number of cells within each

bin. Consistent with our total numbers we could observe a tendency for increased MGE-derived interneuron numbers in the cortex at P19 but not P60 (Figures 3.4 and 3.5 F-O). However, these cells were distributed throughout the cortical layers hence failed to show statistical significance within a specific layer.

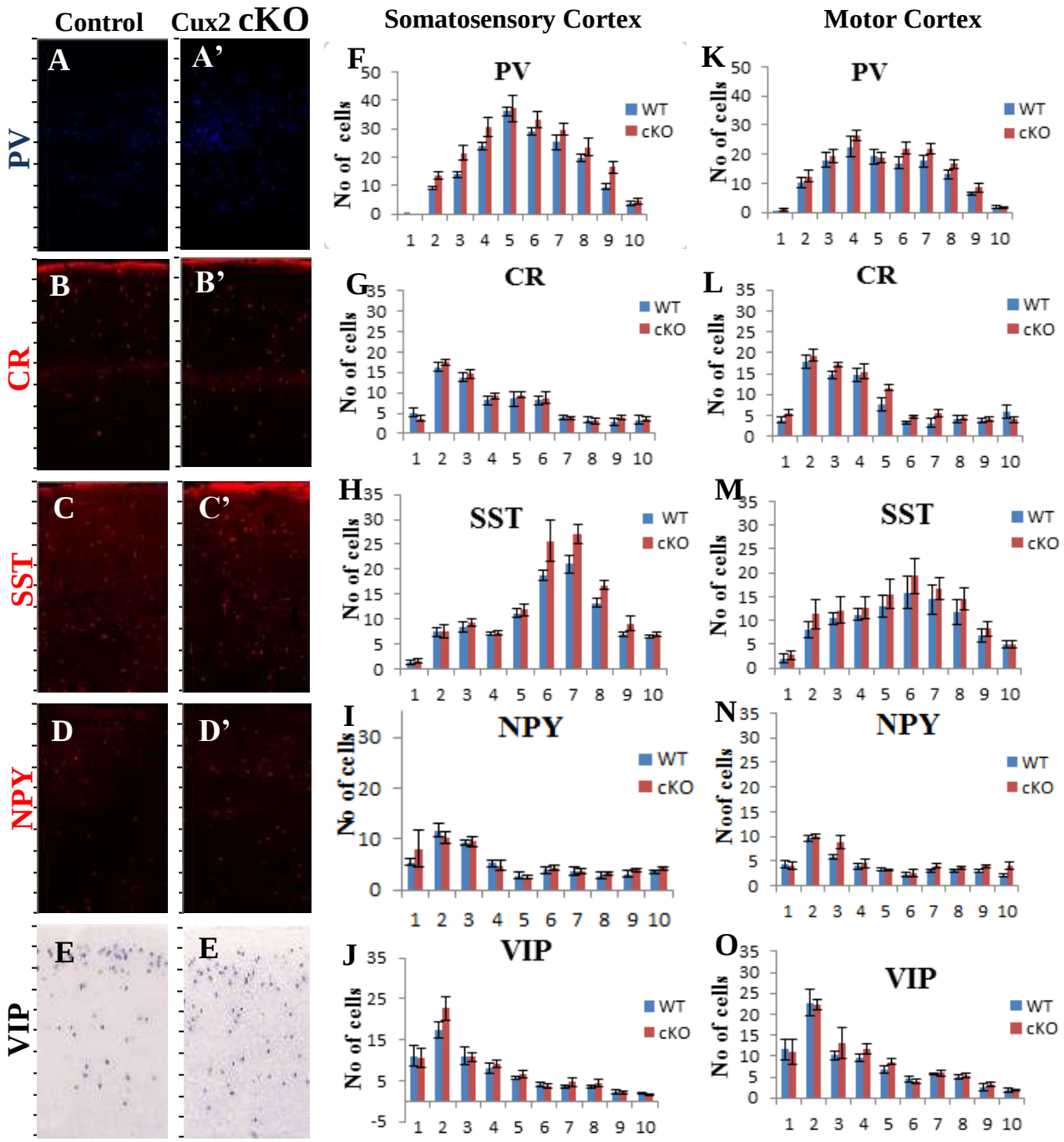

Figure 3.4 The distribution of interneurons across cortical layers at P19. A-E' Images showing the various markers used, the area used for counting and the bin distribution. Immunohistochemistry was used for all the markers except for the VIP for which we used RNA *in situ* hybridization. Bin 1 is near the pial surface and bin 10 is close to the corpus callosum. F-O Quantification of interneuron distribution across layers in the somatosensory cortex (F-J) and motor cortex (K-O).

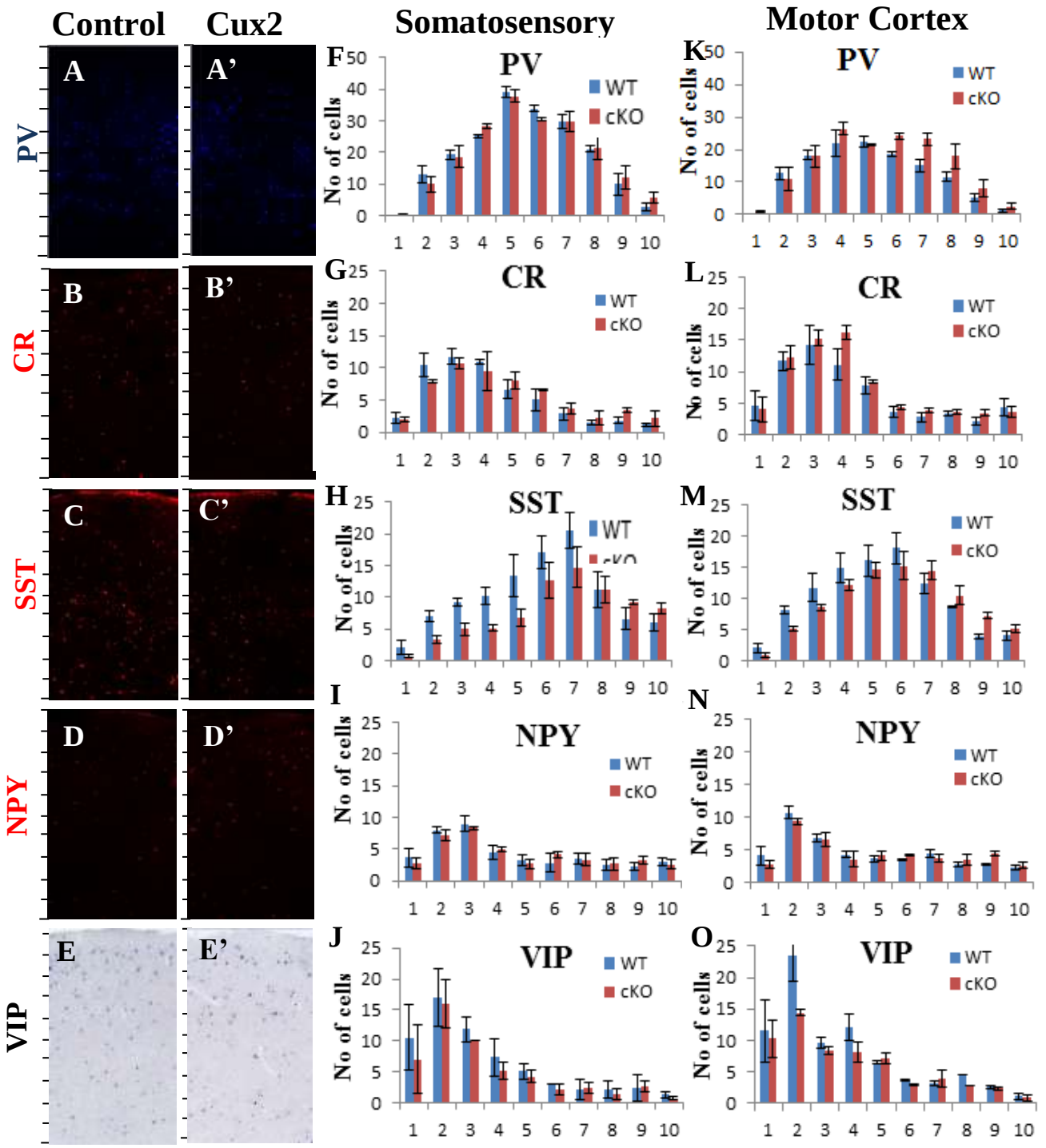

Figure 3.5 The distribution of interneurons across cortical layers at P60. A-E' Images showing the various markers used, the area used for counting and the bin distribution. Immunohistochemistry was used for all the markers except for the VIP for which we used RNA *in situ* hybridization. Bin 1 is near the pial surface and bin 10 is close to the corpus callosum. F-O Quantification of interneuron distribution across layers in the somatosensory cortex (F-J) and motor cortex (K-O).

3.4 Increased numbers of perisomatic and AIS-targeting GABAergic boutons in upper cortical layers in *Cux2* conditional mutant animals.

Given the increased numbers of cortical MGE-derived interneurons at P19, we next addressed the question of whether this results in increased synaptic contacts originating from these supernumerous inhibitory neurons. We examined the total number of inhibitory (Vgat-Gephrin) and excitatory (Vglut-PSD95) appositions in layers I and II/III in control and cKO mice using immunohistochemistry (see materials and methods) (Figure 3.5). Comparison between the two groups of animals failed to reveal a difference between them regarding the total number of GABAergic (Fig. 3.6 A-D, n=3, p=0.6045 for layer 1, p=0.9231 for layers 2-3) or glutamatergic (Fig. 3.6 E-H, n=3, p=0.1287 for layer 1, p=0.0908 for layers 2-3) synapses.

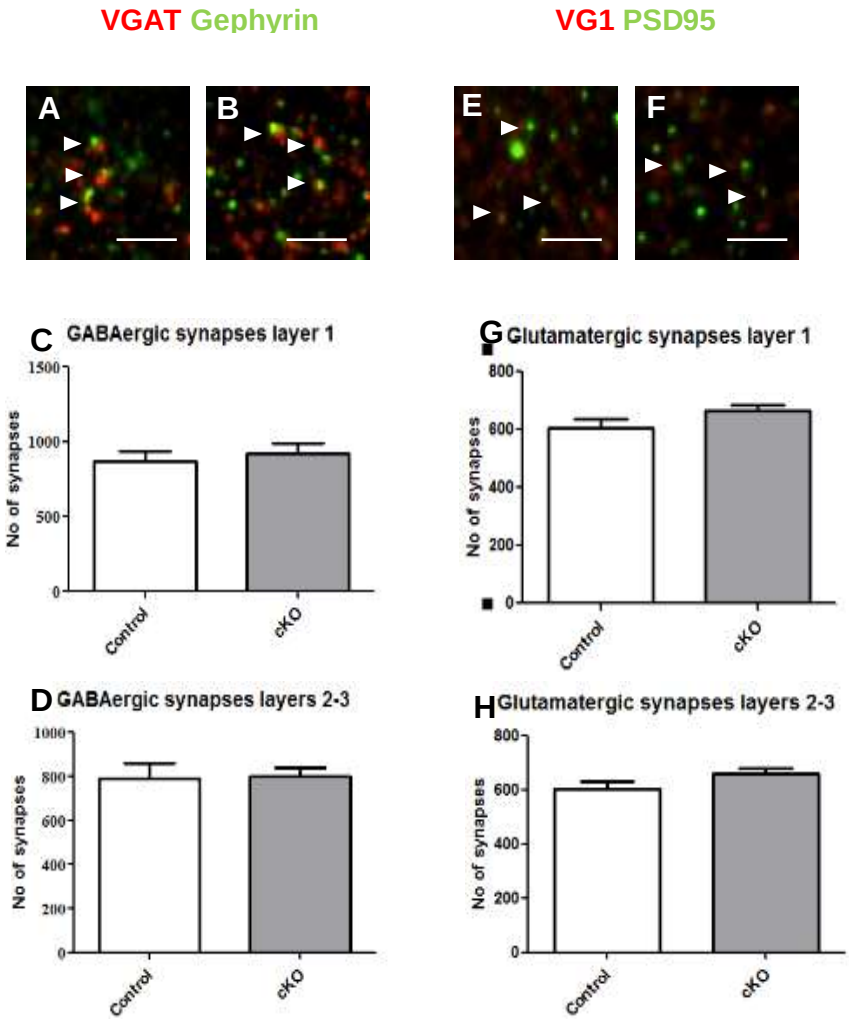

Figure 3.6 The total number of glutamatergic and GABAergic synapses is unaltered in the cortex of *Cux2* cKO mice compared to controls at P19. Images of double staining for GABAergic and glutamatergic synaptic markers. White arrowheads show examples of appositions between pre- and post-synaptic markers. Lens: 63x. The scale bar indicates 4 µm

The axon terminals of PV expressing interneurons target the soma and axon initial segment of pyramidal neurons (Markram 2004). Since the number of PV expressing interneurons is specifically increased in the cortex of *Cux2* cKO mice we investigated whether the

perisomatic and AIS-targeting GABAergic synapses in particular are increased. For this purpose we used immunohistochemistry for the presynaptic marker VGAT (Vesicular GABA Transporter) combined with either an antibody for NeuN, which labels the neuronal cell body, or pIkBa, which labels the axon initial segment. We observed statistically significant incerases in both perisomatic (n=3, p<0.0001) and AIS-targeting (n=3, p=0.0494) boutons (Figures 3.7, 3.8) at P19. At P60 however there was no significant difference between control and cKO mice (n=3, P=0.2664 for perisomatic, p=0.2443 for AIS-targeting), which is consistent to the findings for the interneuron numbers at this age.

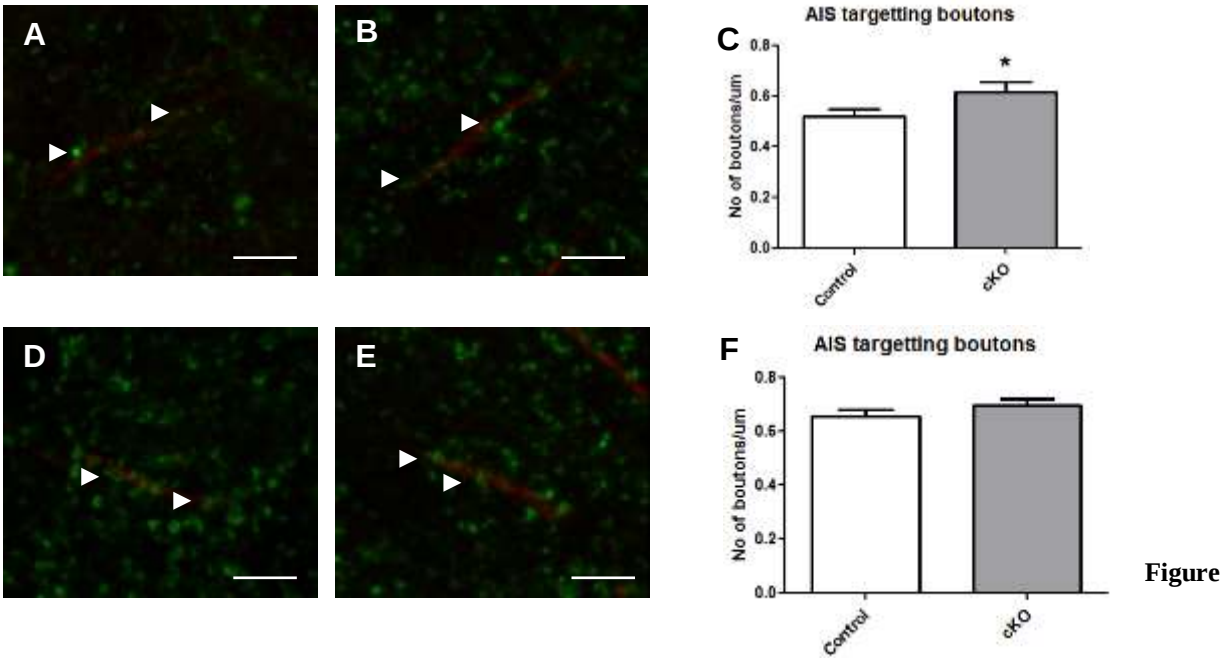

Error! No text of specified style in document..**7 The number of GABAergic boutons per axon initial segment is increased in the cortex of cKO mice at P19 but not at P60. Images of the double staining for AIS-targeting GABAergic boutons. Green staining; VGAT. Red staining: pIkBa. Arrowheads show examples of VGAT puncta in contact with axon initial segments. A, B, C Images and quantification at P19. A) control, B) conditional mutant. D, E, F Images and quantification at P60. D) control E) conditional mutant. Scale bar indicates 6um.**

-

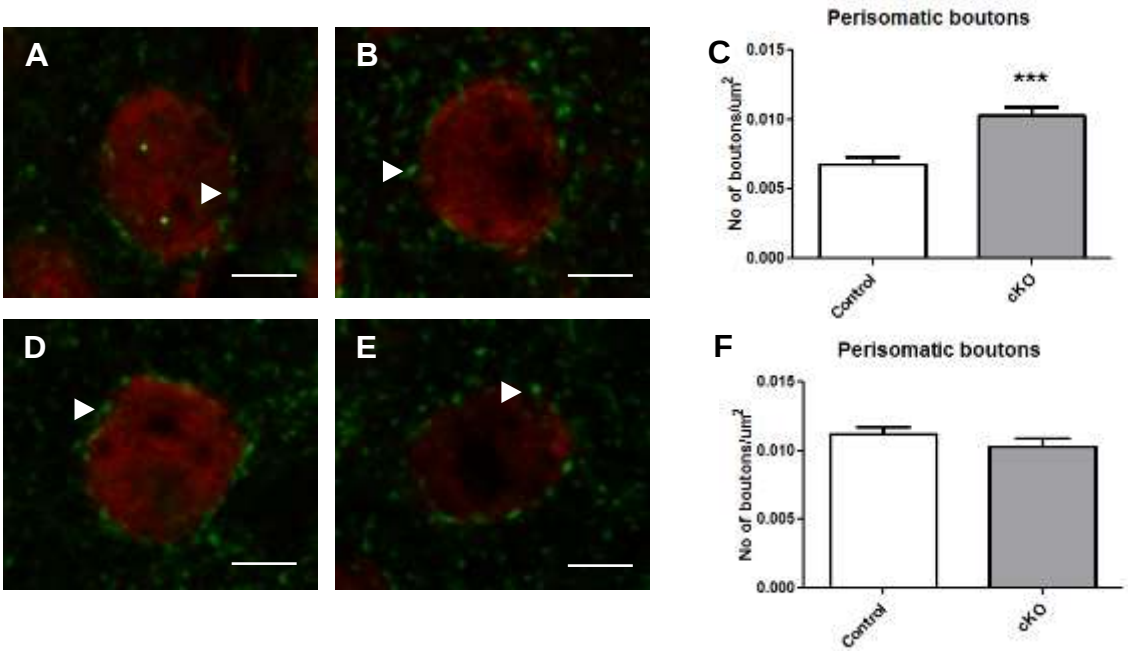

Figure Error! No text of specified style in document.**.8 The number of GABAergic boutons per cell body is increased in the cortex of cKO mice at P19. Images of the double staining for perisomatic GABAergic boutons. Green staining: perisomatic VGAT. Red staining: NeuN. A, B, C Images and quantification at P19. A) Control B) Conditional mutant D, E, F Images and quantification at P60. D: Control E) Conditional mutant. Arrowheads show examples of VGAT puncta in contact with cell bodies. Scale bars indicate 6um.**

3.5 Abnormal electrophysiology in upper cortical layers at P19 in *Cux2* cKO mice

To determine whether the increased number of cortical interneurons and their synaptic contacts that we observed in upper cortical layers result in defective physiology, cortical slices from control and cKO mice were used at P19 to assess miniature inhibitory postsynaptic currents onto pyramidal cells. This work was carried out by a collaborator (Dr Beverley Clark) and did not form part of my Master's project. However, I present the data as they form an integral part of the project. We identified increased frequency and amplitude of miniature inhibitory postsynaptic currents (mIPSCs) in principal cells in *Cux2* cKO mice, consistent with the observed increases in the numbers of cortical interneurons and their synapses onto pyramidal neurons. The intrinsic properties of CUX2-deficient interneurons remained normal (collaboration with Dr Simon Butt, Oxford).

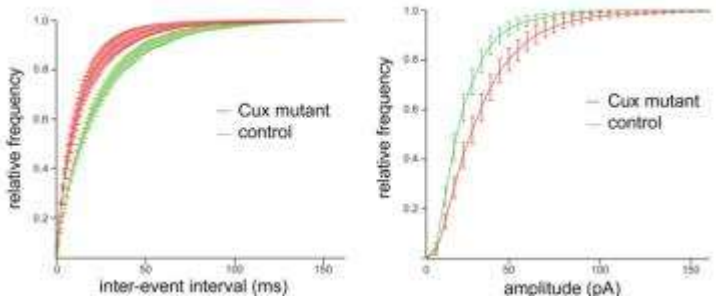

Figure 3.9: Physiological deficits in mice lacking *Cux2* in the MGE. Increased frequency and amplitude of mIPSCs in pyramidal neurons in layers II-III in the somatosensory cortex at P18. p<0.001 K-S-test.

3.6 *Cux2* cKO mice present defects in social behaviour

As increased inhibitory transmission has been observed in mouse models of Autism (as well as Down's Syndrome and Rett Syndrome), we initially assessed sociability in our conditional mutants. For this, Crawley's sociability and social innovation preference test was applied. This test allows the quantification of parameters regarding social recognition in a first stage and social memory and social innovation preference in the second stage (described in detail in Methods and Materials). Abnormal behaviour was observed in the sociability (session 1) stage of the test in the cKO mice at P90. More specifically, the time spent in the empty cage compartment, as well as the number of the contacts with the cage was not different from the respective parameters for the Mouse 1 cage, (number of contacts: p=0.1844, duration of contacts: p=0.01, duration of entries: p=0.3358). This was in contrast to control mice, which preferred the cage containing the stranger mouse, (number of contacts: p=0.0003, duration of contacts: p<0.0001, duration of entries: p=0.0002). This result indicates that mice lacking *Cux2* in cortical interneurons are socially impaired. Locomotor activity on an accelerated rotarod test appeared normal (not shown).

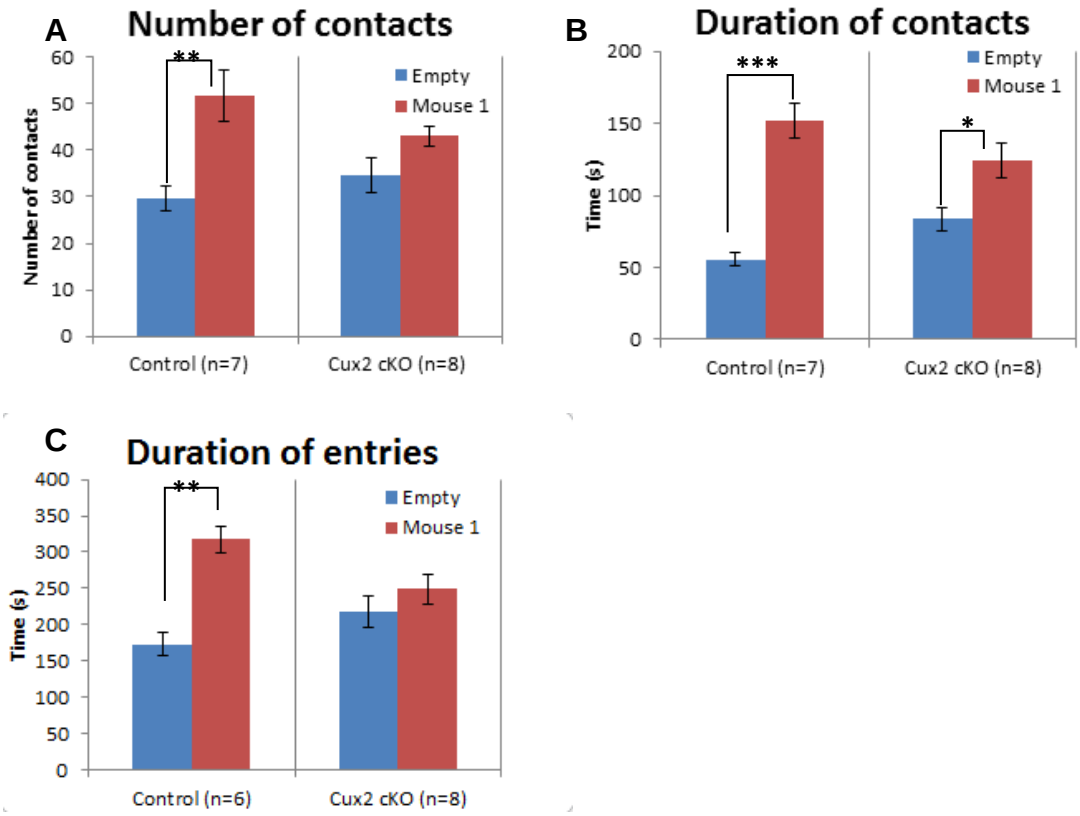

Figure 3.9 : Cux2 cKO mice present defects in sociability. Quantification of parameters scored during the session 1 of Crawley's test in control and cKO animals at P90.

Chapter 4

Discussion

This study aimed at providing insights into the possible functions of CUX2 in the development of interneurons of the cortex. Since the MGE generates the majority of these interneurons we chose to target this area. We used an *Nkx2-1-Cre* mouse, in order to achieve deletion of CUX2 specifically in the MGE while leaving expression outside this area intact. We confirmed the deletion of exons 21-23 of the gene by RNA *in situ* hybridization. Further confirmation that this results in LOF is needed. This could be achieved either by immunohistochemistry for the CUX2 protein or, in the absence of available antibodies, by using $Cux2^{\Delta/\Delta}$ mice to show that they present similar defects to the reported germline LOF mice.

First we checked whether there was an effect of CUX2 loss on the migration of interneurons originating from the MGE. For this purpose we examined the expression of *Lhx6* in conditional mutant and control embryos using RNA *in situ* hybridization. *Lhx6* is a reliable marker of interneurons born in the MGE as its expression persists throughout development and adulthood. This experiment showed that MGE-derived interneurons migrate normally into the cortex and follow the expected tangential migratory streams. More animals need to be used to quantify the number of interneurons migrating at this age and the distance of their migration. This will reveal whether there are any quantitative differences in the development of these cells at embryonic stages.

Several studies have shown that CUX2 may be involved in cell proliferation and cell cycle exit/progression. For example, it affects the proliferation of neuronal stem cells in the olfactory bulb and the intermediate progenitors in the SVZ of the cortex and maintains the interneuron progenitor pool in the spinal cord. It exerts these actions by interfering with the cell cycle and in this way has an impact on the number of mature neurons in the adult CNS. Based on these results we enquired whether it has the same or similar effect on the numbers of the MGE-derived interneurons in the cortex. Our analysis of interneuron markers revealed that, indeed, CUX2 loss in the MGE results in an increase in the numbers of PV^{+ve} interneurons at P19. A similar trend for SST^{+ve} neurons is also observed but this is not statistically significant. This result suggests that, similar to its effects in other CNS regions, CUX2 may be responsible for the negative control of the proliferation of progenitors in the SVZ of the MGE. Staining with the appropriate markers, such as EdU, PH3 and Ki67 would cast light onto any defects in proliferation. Furthermore, given that PV^{+ve} interneurons derive from

the MGE, we can infer that this effect is cell-autonomous. The increase in PV^{+ve} interneurons was present in the somatosensory cortex, but not in the motor cortex, indicating that perhaps the excess number of interneurons born in the MGE of mutant mice do not migrate extensively enough to reach this area of the cortex. We performed the same analysis in controls and mutant mice at P60, but there were no differences between the groups at this age, leading to the hypothesis that homeostatic mechanisms, perhaps cell death, bring the interneuron numbers back to normal after the age of P19. Immunohistochemistry for cell death markers, such as caspases, in ages between P20 and P60 could be a possible way to address this question.

Since the number of GABAergic interneurons in the cortex was increased, we next examined the conditional knockout mice for differences in the number of GABAergic synapses. We failed to see any statistically significant difference in the total number of GABAergic synapses. However, we observed a statistically significant increase in the number of soma- and axon initial segment-targeting GABAergic synapses at P19. This result is consistent with an increase in PV positive interneurons in the cortex at this age, as this population sends its axon terminals to the soma and axon initial segment of pyramidal neurons. At P60 there was no difference between controls and conditional knockouts, which is in agreement with the lack of difference in the numbers of interneurons at this age.

In accordance with an increased number of GABAergic synapses in the cortex of conditional mutants, increased frequency and number of mIPSPs was found in the cortex of the same mice at P19. mIPSP are spontaneous releases of neurotransmitter in the synaptic cleft and hence reflect the number of synapses, rather than the activity of the neurons.

Inhibition is critical for both the development and function of CNS circuits in mammals (Le Magueresse 2013). The balance between inhibition and excitation in the cortex is integral for proper function and aberrations from this balance are a common finding in mouse models for neuropsychiatric and neurodevelopmental disorders (Marin 2012). Increased inhibition in the neocortex has been linked with abberant social behaviour, appearing in autism spectrum disorders in human and in rodent models for autism (Tabuchi 2007, Etherton 2011). Since the conditional knockouts exhibit overinhibition, we tested our conditional mice for defects in social behaviour, using Crawley's sociability test, at P90. In this test the controls preferred a stranger mouse in a cage rather than an empty cage, whereas the mutants did not distinguish between the two, which indicated aberrant social behaviour in these mice. As seen in P60 mice, the number of interneurons is similar to controls at this age so, the behavioural defect cannot be a direct outcome of overinhibition. It has been shown that GABA mediated inhibition is very important for the initiation of critical periods of

plasticity, mostly in the visual cortex (Le Magueresse et al. 2013). Moreover, transplantation of inhibitory interneuron precursors in the visual cortex induced ocular dominance plasticity after the critical period was over (Southwell et al. 2010). Hence, a possible explanation would be that the increased GABA transmission at early postnatal stages causes alterations in the surrounding network that persist until later in life. Electrophysiological analysis of older animals should reveal possible aberrations in the network that may underlie abnormal behaviour.

References

Allène, C. et al., 2008. Sequential generation of two distinct synapse-driven network patterns in developing neocortex. *The Journal of neuroscience : the official journal of the Society for Neuroscience*, 28(48), pp.12851–63.

Anastasiades, P.G. & Butt, S.J.B., 2011. Decoding the transcriptional basis for GABAergic interneuron diversity in the mouse neocortex. *The European journal of neuroscience*, 34(10), pp.1542–52.

Andres, V., Nadal-ginard, B. & Mahdavi, V., 1992. Clox , a mammalian homeobox gene related to Drosophila cut , encodes DNA-binding regulatory proteins differentially expressed during development. *Development*, 334, pp.321–334.

Behar, T.N. et al., 1998. Differential Response of Cortical Plate and Ventricular Zone Cells to GABA as a Migration Stimulus. , 18(16), pp.6378–6387.

Blochlinger, K. et al., 1990. Patterns of expression of Cut , a protein required for external sensory organ development in wild-type and cut mutant Drosophila embryos. *Genes and Development*, 4, pp.1322–1331.

Blochlinger, K., Jan, L.Y. & Jan, Y.N., 1991. Transformation of sensory organ identity by ectopic expression of Cut in Drosophila. *Genes & Development*, 5(7), pp.1124–1135.

Bodmer, R. et al., 1997. Transformation of Sensory Organs by Mutations of the cut Locus of D . melanogaster. *Cell*, 51, pp.293–307.

Bortone, D. & Polleux, F., 2009. KCC2 expression promotes the termination of cortical interneuron migration in a voltage-sensitive calcium-dependent manner. *Neuron*, 62(1), pp.53–71.

Brochlinger, K. et al., 1988. Primary structure and expression of a product from cut, a locus involved in specifying sensory organ identity in Drosophila. *Nature*, 333, pp.629–635.

Campbell, K., 2003. Dorsal-ventral patterning in the mammalian telencephalon. *Current Opinion in Neurobiology*, 13(1), pp.50–56.

Cancedda, L. et al., 2007. Excitatory GABA action is essential for morphological maturation of cortical neurons in vivo. *The Journal of neuroscience : the official journal of the Society for Neuroscience*, 27(19), pp.5224–35.

Cobos, I. et al., 2006. Cellular patterns of transcription factor expression in developing cortical interneurons. *Cerebral cortex (New York, N.Y. : 1991)*, 16 Suppl 1, pp.i82–8.

Cubelos, B. et al., 2010. Cux1 and Cux2 regulate dendritic branching, spine morphology, and synapses of the upper layer neurons of the cortex. *Neuron*, 66(4), pp.523–35.

Cubelos, B. et al., 2008. Cux-2 controls the proliferation of neuronal intermediate precursors of the cortical subventricular zone. *Cerebral cortex (New York, N.Y. : 1991)*, 18(8), pp.1758–70.

Del Rio JA, Soriano E, Ferrer I., 1992. Development of GABA-immunoreactivity in the neocortex of the mouse. *J Comp Neurol*, 326(4), pp501-26

Defelipe, J. & As, I.F., 1992. The pyramidal neuron of the cerebral cortex: morphological and chemical characteristics of the synaptic inputs. *Progress in neurobiology*, 39, pp.563–607.

Douglas, R. & Martin, K., 1982. Neocortex. In *The synaptic organization of the brain*. pp. 459–509.

Faux, C. et al., 2010. Differential gene expression in migrating cortical interneurons during mouse forebrain development. *The Journal of comparative neurology*, 518(8), pp.1232–48.

Fernando, R.N. et al., 2011. Cell cycle restriction by histone H2AX limits proliferation of adult neural stem cells. *Proceedings of the National Academy of Sciences of the United States of America*, 108(14), pp.5837–42.

Flames, N. et al., 2007. Delineation of multiple subpallial progenitor domains by the combinatorial expression of transcriptional codes. *The Journal of neuroscience : the official journal of the Society for Neuroscience*, 27(36), pp.9682–95.

Franco, S.J. et al., 2012. Fate-restricted neural progenitors in the mammalian cerebral cortex. *Science (New York, N.Y.)*, 337(6095), pp.746–9.

Freund, T.F., 2003. Interneuron Diversity series: Rhythm and mood in perisomatic inhibition. *Trends in neurosciences*, 26(9), pp.489–95.

Gelman, D.M., Marin, O. & Rubenstein, J.L.R., 2012. The generation of cortical interneurons. *Jasper's basic mechanisms of the epilepsies*.

Gupta, A., Wang, Y. & Markram, H., 2000. Organizing Principles for a Diversity of GABAergic Interneurons and Synapses in the Neocortex. *Science*, 287(5451), pp.273–278.

Heuvel, G.B. Vanden et al., 1996. Expression of a cut-related homeobox gene in developing and polycystic mouse kidney. *Kidney International*, 50, pp.453–461.

Iulianella, A. et al., 2008a. Cux2 (Cutl2) integrates neural progenitor development with cell-cycle progression during spinal cord neurogenesis. *Development (Cambridge, England)*, 135(4), pp.729–41.

Iulianella, A. et al., 2008b. Cux2 (Cutl2) integrates neural progenitor development with cell-cycle progression during spinal cord neurogenesis. *Development (Cambridge, England)*, 135(4), pp.729–41.

Iulianella, A. et al., 2009. Cux2 functions downstream of Notch signaling to regulate dorsal interneuron formation in the spinal cord. *Development (Cambridge, England)*, 136(14), pp.2329–34.

Iulianella, A., Vanden Heuvel, G. & Trainor, P., 2003. Dynamic expression of murine Cux2 in craniofacial, limb, urogenital and neuronal primordia. *Gene Expression Patterns*, 3(5), pp.571–577.

Jinushi-Nakao, S. et al., 2007. Knot/Collier and cut control different aspects of dendrite cytoskeleton and synergize to define final arbor shape. *Neuron*, 56(6), pp.963–78.

Kawaguchi, Y. & Kubota, Y., 1997. GABAergic Cell Subtypes and their Synaptic Connections in Rat Frontal Cortex. *Cerebral Cortex*, 7, pp.476–486.

Kessaris, N. et al., 2014. Genetic programs controlling cortical interneuron fate. *Current opinion in neurobiology*, 26, pp.79–87.

López-bendito, G. et al., 2003. Blockade of GABA B Receptors Alters the Tangential Migration of Cortical Neurons. *Cerebral Cortex*, 13, pp.932–942.

Magueresse, C. Le & Monyer, H., 2013. Review GABAergic Interneurons Shape the Functional Maturation of the Cortex. *Neuron*, 77, pp.388–405.

Manent, J.-B. et al., 2005. A noncanonical release of GABA and glutamate modulates neuronal migration. *The Journal of neuroscience : the official journal of the Society for Neuroscience*, 25(19), pp.4755–65.

Marin, O & Rubenstein, JL., 2003. Cell migration in the forebrain. *Annu. Rev. Neuroci.,* 26, pp.441-83.

Markram, H. et al., 2004. Interneurons of the neocortical inhibitory system. *Nature reviews. Neuroscience*, 5(10), pp.793–807.

Mataga, N., Mizuguchi, Y. & Hensch, T.K., 2004. Experience-Dependent Pruning of Dendritic Spines in Visual Cortex by Tissue Plasminogen Activator. *Neuron*, 44, pp.1031–1041.

Miyoshi, G. & Fishell, G., 2011. GABAergic interneuron lineages selectively sort into specific cortical layers during early postnatal development. *Cerebral cortex (New York, N.Y. : 1991)*, 21(4), pp.845–52.

Mohajerani, M.H. et al., 2007. Correlated network activity enhances synaptic efficacy via BDNF and the ERK pathway at immature CA3 – CA1 connections in the hippocampus. *PNAS*, 104(32), pp.13176–13181.

Nieto, M. et al., 2004. Expression of Cux-1 and Cux-2 in the subventricular zone and upper layers II-IV of the cerebral cortex. *The Journal of comparative neurology*, 479(2), pp.168–80.

Oray, S., Majewska, A. & Sur, M., 2004. Dendritic Spine Dynamics Are Regulated by Monocular Deprivation and Extracellular Matrix Degradation. *Neuron*, 44, pp.1021–1030.

Quaggin, S.E., Yeger, H. & Igarashi, P., 1997. Antisense Oligonucleotides to Cux-1 , a Cut - related Homeobox Gene , Cause Increased Apoptosis in Mouse Embryonic Kidney Cultures. *Journal of clinical Investigation*, 99(4), pp.718–724.

Valarché, I., Hirsch, M. & Martinez, S., 1993. The mouse homeodomain protein Phox2 regulates Ncam promoter activity in concert with Cux / CDP and is a putative determinant of neurotransmitter phenotype. *Development*, 896, pp.881–896.

Wang, D.D. & Kriegstein, A.R., 2011. Blocking early GABA depolarization with bumetanide results in permanent alterations in cortical circuits and sensorimotor gating deficits. *Cerebral cortex (New York, N.Y. : 1991)*, 21(3), pp.574–87.

Wang, D.D. & Kriegstein, A.R., 2008. GABA regulates excitatory synapse formation in the neocortex via NMDA receptor activation. *The Journal of neuroscience : the official journal of the Society for Neuroscience*, 28(21), pp.5547–58.

Whittington, M. a & Traub, R.D., 2003. Interneuron diversity series: inhibitory interneurons and network oscillations in vitro. *Trends in neurosciences*, 26(12), pp.676–82.

Yang, J.-W. et al., 2013. Thalamic network oscillations synchronize ontogenetic columns in the newborn rat barrel cortex. *Cerebral cortex (New York, N.Y. : 1991)*, 23(6), pp.1299–316.

Zimmer, C. et al., 2004. Dynamics of Cux2 expression suggests that an early pool of SVZ precursors is fated to become upper cortical layer neurons. *Cerebral cortex (New York, N.Y. : 1991)*, 14(12), pp.1408–20.